Published in final edited form as:
*Biochemistry*. 2013 April 2; 52(13): 2328–2336. doi:10.1021/bi400014t.

# Dissecting the Paclitaxel-Microtubule Association: Quantitative Assessment of the 2′-OH Group†

**Shubhada Sharma**[‡], **Chandraiah Lagisetti**[§,†], **Barbara Poliks**[||], **Robert M. Coates**[§], **David G. I. Kingston**[⊥], and **Susan Bane**[‡,*]

[‡]Department of Chemistry, Binghamton University, State University of New York, Binghamton, New York 13902

[§]Department of Chemistry, University of Illinois, Urbana-Champaign, Illinois 61801

[||]Department of Physics, Binghamton University, State University of New York, Binghamton, New York 13902

[⊥]Department of Chemistry, Virginia Tech, Blacksburg, Virginia 24061

## Abstract

Paclitaxel (PTX) is a microtubule-stabilizing agent that is widely used in cancer chemotherapy. This structurally complex natural product acts by binding to β-tubulin in assembled microtubules. The 2′-hydroxyl group in the flexible side chain of PTX is an absolute requirement for activity, but its precise role in the drug-receptor interaction has not been specifically investigated. The contribution of the 2′-OH group to the affinity and tubulin-assembly efficacy of PTX has been evaluated through quantitative analysis of PTX derivatives possessing side chain deletions: 2′-deoxy-PTX, *N*-debenzoyl-2′-deoxy-PTX and baccatin III. The affinity of 2′-deoxy-PTX for stabilized microtubules was more than 100-fold less than that of PTX and only about 3-fold greater than the microtubule affinity of baccatin III. No microtubule binding activity was detected for the analog N-debenzoyl-2′-deoxy-PTX. The tubulin-assembly efficacy of each ligand was in concordance with the microtubule binding affinity, as was the trend in cytotoxicities. Molecular dynamics simulations revealed that the 2′-OH group of PTX can form a persistent hydrogen bond with D26 within the microtubule binding site. The absence of this interaction between 2′-deoxy-PTX and the receptor can account for the difference in binding free energy. Computational analyses also provide a possible explanation for why N-debenzoyl-2′-deoxy-PTX is inactive, in spite of the fact that it is essentially a substituted baccatin III. We propose that the hydrogen bonding interaction between the 2′-OH group and D26 is the most important stabilizing interaction that PTX forms with tubulin in the region of the C-13 side chain. We further hypothesize that the substituents at the 3′-position function to orient the 2′-OH group for a productive hydrogen bonding interaction with the protein.

The diterpenoids paclitaxel (PTX, Taxol®) and docetaxel (TXT, Taxotere®) are highly effective drugs for the treatment of a variety of cancers. PTX, TXT and related taxanes act by interfering with cellular microtubule dynamics through binding to β-tubulin.(1) PTX was the first substance found to bind to microtubules and stabilize them against disassembly.(2) The clinical success of PTX and TXT prompted many studies of structure-activity relationships in this class and searches for other molecular entities that display PTX-like

†Financial support was provided by the National Institutes Health (Grant No. CA-69571).

*To whom correspondence should be addressed: Phone: 607-777-2927. Fax: 607-777-4478. sbane@binghamton.edu.
†Current address: Chemical Biology & Therapeutics, St. Jude Children's Research Hospital 262 Danny Thomas Pl., MS 1000, Memphis, TN 38105

activity. One of these classes of molecules, the epothilones, seems particularly promising. For example, the epothilone derivative ixabepilone (Ixempra®) is approved by the United States Food and Drug Administration for the treatment of breast cancer. Still, the taxane class of molecules continues to be explored for new anticancer agents, with a half dozen PTX-related molecules in various stages of clinical trials.(3)

The first crystallographic structure of tubulin was a breakthrough not only in the understanding of the protein, but also into the molecular mechanism of PTX's interaction with microtubules.(4) Binding to a site facing the microtubule lumen, PTX locks tubulin into its active, "straight" conformation, strengthening contacts between protofilaments and tubulin dimers in the microtubule lattice. The precise binding mode of PTX could not be ascertained from the original data, however. The rigid core of the molecule was visualized, but the binding site conformation of the flexible C-13 side chain could not be clearly delineated. The C-13 side chain of PTX is critical for its antitumor activity, and therefore understanding the interactions between this portion of the molecule and the protein are of utmost importance in understanding precisely how this drug works on a molecular level. Subsequent molecular modeling combined with the electron crystallography density data led to the proposal of the "T-Taxol" model of the microtubule-bound ligand.(5) Experimental data in support of this conformation for the tubulin bound ligand have been presented, (6–8) but it is not universally accepted.(9–11)

Many of the so-called "second generation" taxanes differ from PTX and TXT in the C-13 side chain. (See Figure 1 for PTX structure and numbering system.) Provided that the correct absolute configuration of the C-3′ position is maintained, the substituents on the C-3′ amide and the C-3′ carbon can be replaced with a variety of hydrophobic groups, yielding highly active taxanes.(11) The hydroxyl substituent on the C-2′ position, however, is absolutely essential. Acetylation completely abolishes PTX binding to microtubules (12). Replacing the hydroxyl group with fluorine or thiol decreases cytotoxicity of the PTX by two orders of magnitude.(13, 14) It has long been assumed that the 2′-OH participates in an important hydrogen bonding interaction between the ligand and the protein. To date, though, the precise role of the critical 2′-hydroxyl group in the association and activity of PTX has not been directly addressed.

In the present study, we have quantified the role of 2′-OH group in the affinity and efficacy of PTX to tubulin. We have synthesized two "deletion" PTX derivatives: 2′-deoxy-PTX, which lacks the 2′-OH group, and N-debenzoyl-2′-deoxy-PTX, which lacks both the 2′-OH and the 3′-benzoyl group. Their affinities for GMPcPP-stabilized microtubules, their efficacies as promoters of pure tubulin assembly, and their cytoxicities have been measured and compared with those of the parent molecule, PTX, and the paclitaxel derivative devoid of the side chain, baccatin III. We find that the 2′-OH accounts for 80% of the binding free energy of the entire side chain. Therefore, the 2′-OH is energetically and functionally the most important component of the side chain; the lack of the hydroxyl group renders 2′-deoxy-PTX more like baccatin III than PTX in activity. Somewhat surprisingly, we could detect no microtubule binding or cytotoxicity for the double deletion derivative N-debenzoyl-2′-deoxy-PTX at concentrations up to its maximum solubility. In this case, the presence of the partial side chain at C-13 is more deleterious to microtubule binding than its complete absence.

Computational analyses were performed to understand the behavior of these molecules. Molecular dynamic simulations were performed for PTX and N-debenzoyl-2′-deoxy-PTX within the binding site in the 1JFF (15) as well as T-Taxol-tubulin (5) structures. These results confirm the expected presence of a hydrogen bonding interaction between the 2′-OH and the protein, but our model identifies D26 as the primary hydrogen bond acceptor in the

binding site, which has not heretofore been emphasized in this role. The modeling results also provide an explanation for how a PTX derivative with a side chain can be much less active than baccatin III, the derivative that has no side chain at all.

## MATERIALS AND METHODS

All chemicals used were analytical grade and purchased from Sigma Chemicals unless mentioned otherwise. The compounds 2′-deoxy-PTX and N-debenzoyl-2′-deoxy-PTX were synthesized based on methods of Walker *et al.* (16) and Long et al..(17) N-AB-PT and GMPcPP were previously synthesized.(18) Stock solutions of all taxanes were made in DMSO. All references to percent DMSO concentration are v/v. The concentrations of N-debenzoyl-2′-deoxy-PTX, 2′-deoxy-PTX and PTX were determined in DMSO using $\varepsilon_{273\ nm,\ DMSO} = 1.7 \times 10^3\ M^{-1}cm^{-1}$ (19) and the concentrations of baccatin III and N-AB-PT were determined using $\varepsilon_{276nm,\ DMSO} = 1.19 \times 10^3\ M^{-1}cm^{-1}$ for baccatin III (20) and $\varepsilon_{320nm,\ DMSO} = 2.08 \times 10^3\ M^{-1}cm^{-1}$ for N-AB-PT, respectively (18).

### Tubulin Purification and Protein Determination

Tubulin was prepared by two cycles of temperature dependent assembly-disassembly followed by ion exchange chromatography (21). The purified tubulin was drop frozen in liquid nitrogen. Prior to use, the frozen pellets were gently thawed and then desalted into PME buffer (100 mM PIPES, 1 mM $MgSO_4$, and 2 mM EGTA, pH 6.90 at 25 °C) by the method of Penefsky (22). The concentration of tubulin was determined spectrophotometrically on a Hewlett Packard Model 8453 diode array spectrophotometer using an extinction coefficient of 1.23 $(mg/mL)^{-1}cm^{-1}$ at 278 nm.

### Promotion of Tubulin Assembly

Tubulin assembly was monitored by apparent absorption at 350 nm using a Hewlett-Packard 8453 absorption spectrophotometer with a multicell holder that was maintained at 37 °C with a circulating water bath. Tubulin in PME buffer containing 0.1 mM GTP was equilibrated at 37 °C in the spectrophotometer and a baseline was recorded. Assembly was initiated by adding the taxane in DMSO. The progress of the reaction was monitored by the increase in apparent absorption at 350 nm as a function of time until a steady state was reached. The extent of microtubule assembly was determined as the difference between the apparent absorption at steady state and that at the baseline. The concentration of DMSO was maintained at 4% or less depending upon the requirement of the experiments.

### Preparation of GDP-tubulin and GMPcPP-tubulin

GDP-tubulin and GMPcPP-tubulin, in which the E-site nucleotide is fully replaced by GDP or GMPcPP, respectively, were prepared as described previously (23, 24). Unbound GDP and excess GMPcPP were not removed from the system.

### Affinity of Ligands for GMPcPP-Microtubules

The affinity of taxanes for GMPcPP-stabilized microtubules was assessed by competition with a fluorescent derivative of PTX, NAB-PT, as described previously (7) with the following modifications. The concentrations of GMPcPP microtubules and N-AB-PT were 1 μM each instead of 5 μM, and the concentration of DMSO in the experiments was 15% (25) instead of 4% owing to the low solubility of the compounds. The fluorescence emission spectrum of each sample was collected on a Jobin Yvon FluoroMax3 spectrofluorometer (excitation wavelength = 320 nm) in a cell holder maintained at 37 °C. A 2 ×10 mm quartz cuvette was used for the measurements and was oriented such that the excitation beam passed through the short path. Appropriate background spectra were subtracted before data

analysis. $EC_{50}$ values of ligands for GMPcPP-microtubules were determined by a plot of ($F/F_0$) versus the log of the taxane concentration, where $F_0$ is fluorescence emission intensity at 413 nm of N-AB-PT bound to GMPcPP-microtubules in the absence of non-fluorescent analogs and F is the fluorescence emission intensity at 413 nm of N-AB-PT in the presence of a given concentration of the non-fluorescent ligand. An inhibition constant (Ki) for each ligand was determined using a one-site competition relation: $Ki = EC_{50}/(1+[\text{N-AB-PT}]/K_{PTX})$, where $K_{PTX}$ is the dissociation constant for N-AB-PT with GMPcPP-polymerized tubulin (15 nM, (23)), and [N-AB-PT] is 1 μM. The inhibition constant reflects the relative dissociation constant (Kd) or association constant (1/Kd) for the non-fluorescent ligand binding to microtubules.

## Critical Concentration Determination

Critical concentrations ($C_{crit}$) of tubulin assembly in the presence of PTX, 2′-deoxy-PTX or baccatin III were determined by assembly experiments in PME buffer containing 2% DMSO performed at 37 °C. Various concentrations of tubulin in PME buffer (containing 2% DMSO) were polymerized with the ligands and the extent of assembly was measured. Tubulin:ligand concentration ratios of 1:0.5, 1:1 and 1:1.3 were used for PTX, 2′-deoxy-PTX, and baccatin III, respectively. Critical concentrations were obtained as the *x*-intercepts of plots of apparent absorption at 350 nm at steady state ($\Delta A_{350nm}$) versus tubulin concentration.

## Determination of Cytotoxicity

PC3 cells were grown in HAMS F-12K medium supplemented to 10% fetal bovine serum and maintained in a humidified atmosphere of 5% $CO_2$ in air at 37 °C. The cytotoxicity assay was performed based on the method of Skehan *et al.*. (26) $IC_{50}$ values were obtained from plots of the absorbance of SRB at 570 nm vs. the concentration of taxane.

## Computational Simulations of PTX and N-debenzoyl-2′-deoxy-PTX

Computational simulations involving PTX were performed on 1JFF (15) and T-Taxol-tubulin structures. The file 1JFF was downloaded from the RSCB Protein Data Bank. The structure of T-Taxol-tubulin was created using coordinates from the Supplement to (27). The structure of tubulin-bound N-debenzoyl-2′-deoxy-PTX was created from 1JFF by removing the 2′-OH group and N-benzoyl group of PTX.

Computational simulations for all the structures described above were performed using AMBER 9, a suite of programs for molecular dynamics simulations of proteins and nucleic acids, developed by The Scripps Research Institute (TSRI) [The Scripps Research Institute, The AMBER Molecular Dynamics Package. http://amber.scripps.edu]. Visualization and manipulation of the structures were performed using either DS Visualizer or Insight II Viewer (Accelrys, San Diego).

The AMBER force field (2003 version) was used for the protein and water and the force field parameters for the ligands (PTX, GTP and GDP) were obtained from GAFF (general AMBER force field). The partial charges for the ligands (PTX, GTP and GDP) were calculated using the electrostatic potential (ESP) fit method in DMol3 module of the Materials Studio 4.1 software by Accelrys San Diego (28). Each system was neutralized by adding 31 $Na^+$ ions and was immersed in TIP3P box of water (29) extending 15 Å from the surface of the protein and periodic boundary conditions were applied.

All the structures mentioned at the beginning of this section were equilibrated for 120 picoseconds at 300 K with 1g/$cm^3$ water density and minimized. Additionally, for the two PTX structures equilibration was followed by a long term (10 nanoseconds) dynamics

session and the time evolution of the distances between the 2′-OH group from side chain oxygens of D26 as well as the backbone amides of G370 and R369, respectively, were recorded for each structure.

# RESULTS

## Tubulin-Assembly Activity of PTX Analogs

Initial assessment of *in vitro* activity of the taxanes was performed by measuring tubulin assembly in the presence of PTX and the other molecules (Figure 2). Like PTX, 2′-deoxy-PTX induces tubulin to assemble into normal microtubules (confirmed by electron microscopy, data not shown). Baccatin III is weakly active, but *N*-debenzoyl-2′-deoxy-PTX does not promote tubulin assembly under these conditions.

## Relative Binding Affinity for Stabilized Microtubules

Polymerization assays do not provide a direct assessment of a ligand's affinity for tubulin owing to the linkage between tubulin binding and microtubule assembly.(30) Association constants for assembly-promoting ligands binding to microtubules can be determined under conditions in which the concentration of polymerized tubulin is essentially constant, such as with crosslinked microtubules (31) or with GMPcPP-microtubules.(32) Most quantitative evaluations of equilibrium binding parameters for PTX-site ligands have been performed by measuring displacement of a fluorescent PTX bound to stabilized microtubules.(33) In this investigation, the apparent equilibrium constants for the PTX derivatives were assessed using GMPcPP-stabilized microtubules and the fluorescent PTX analog N-debenzoyl-N-(*m*-aminobenzoyl)paclitaxel (N-AB-PT) as the reporter ligand. The competition curves are shown in Figure 3. Curves for the ligands other than PTX are truncated at the maximum solubility of each ligand under the experimental conditions (15% DMSO in PME buffer). It is seen that removal of the 2′-OH group shifts the binding curve to the right of PTX, closer to that of baccatin III than to PTX. No inhibition of N-AB-PT binding to microtubules was observed with N-debenzoyl-2′-deoxy-PTX at its highest soluble concentration, 45 μM. The apparent association constants for the taxanes binding to GMPcPP-microtubules at 37 °C, calculated as described under *Materials and Methods*, are listed in Table 1. Note that the apparent association constants for PTX and baccatin III binding to microtubules under these conditions are in good agreement with literature values (31, 34), confirming that the high concentration of DMSO in this assay does not adversely affect the results (25). Binding free energies were calculated from the apparent association constants. These values are listed in Table 1.

## Tubulin Assembly Efficacy of Taxanes

The efficacies of PTX, 2′-deoxy-PTX and baccatin III were measured in terms of their effect on the critical concentration ($C_{crit}$) of tubulin assembly (Figure 4). $C_{crit}$ of tubulin assembly is the minimum concentration of tubulin required for microtubule formation under a particular set of experimental conditions (35). The inverse of $C_{crit}$ is a good approximation of the apparent elongation constant ($K_p$) for tubulin assembly. The apparent elongation constant is a measure of the affinity of the growing microtubule end for an unassembled tubulin dimer.

Critical concentrations were determined by measuring microtubule assembly caused by the ligands at varying concentrations of protein in the presence of 2% DMSO (Figure 4). Since there was no detectable binding of 2′-deoxy-3′-debenzoyl-PTX to tubulin in the competition assay, this ligand was excluded from the experiments. Ideally, critical concentration measurements should be performed under conditions in which the PTX binding site is saturated with ligand. Unfortunately, 2′-deoxy-PTX is insufficiently soluble

for this protocol. Instead, critical concentrations were measured at ligand:tubulin concentration ratios that provide the same fractional occupation of the PTX binding site based on the apparent equilibrium constants determined here for taxane binding to GMPcPP microtubules. Tubulin:taxane concentration ratios used were 1:0.5 for PTX, 1:1 for 2′-deoxy-PTX, and 1:1.3 for baccatin III. The critical concentration of tubulin in the absence of promoter was also measured. Critical concentrations and the corresponding elongation constants and free energies of elongation are listed in Table 2. Under these experimental conditions, PTX lowers the critical concentration of tubulin by a factor of 9, which corresponds to a difference in free energy of elongation of 1.3 kcal/mol. About half of this free energy difference is lost by removal of the 2′-OH group.

## Cytotoxicity of Taxanes

Cytotoxicities of taxanes in PC3 cells are listed in Table 4. As expected, 2′-deoxy-PTX is much less cytotoxic than PTX. A comparison of the relative cytotoxicities of the four taxanes is revealing. PTX is 350-fold more cytotoxic than 2′-deoxy-PTX, but 2′-deoxy-PTX is only about 6-fold more cytotoxic than baccatin III. Again, removal of just the 2′-OH group is almost as deleterious to activity as removal of the entire side chain, and removal of both the 2′-OH and 3′-benzoyl group renders the molecule inactive.

## Computational Analysis of the 2′-OH group and N-benzoyl group of PTX

Possible binding site interactions between PTX and tubulin were probed by molecular dynamics simulations. Two different initial structures were studied: 1JFF (coordinates from the PDB) and T-taxol-tubulin (coordinates from the Supplementary Material of Alcaraz *et al.*(27)). The structures were minimized as described under *Materials and Methods*, and amino acid residues within 6 Å of the 2′-oxygen and the 3′-nitrogen of PTX were identified (Figure 5A and B). Except for the orientation of the 3′-benzamide, the two minimized structures are very similar. The 2′-OH is within hydrogen bonding distance of three possible donors: backbone nitrogens of R369 and G370, previously noted by Snyder *et al.* (5), and a side chain oxygen of D26, which has not been explicitly implicated in binding site models of PTX. In order to evaluate the candidates participating in hydrogen bonding interaction with the 2′-OH, the two structures were subjected to long term dynamics (10 ns, described under *Materials and Methods*) and the time evolution of the distances of the 2′-OH group from side chain of D26 and the backbone amides of G370 and R369 were recorded (Figure 6). In the JFF structure, the distances between the peptide bond nitrogens and the 2′-oxygen are essentially constant over the period, while the carboxylate oxygens are quickly displaced outside of typical hydrogen bonding distance. In contrast, in the T-Taxol structure the closest distance over the dynamics period is between the 2′-oxygen and one of the carboxylate oxygens of D26. The carboxylate oxygens exchange positions with one another twice during the simulation. The amide nitrogen of G370 remains within about 4 Å of the 2′-OH, while the amide nitrogen of R349 moves to more than 5 Å away from the 2′-OH.

The binding site within 6Å of the 3′-nitrogen of PTX in 1JFF comprised of R369, G370, P360, D26, H229, A233 and V23. The side chain of D26 was found to be at 3.1Å from this nitrogen. In the complex of N-debenzoyl-2′-deoxy-PTX equilibrated with tubulin, the unsubstituted 3′-amino group flipped away from the side chain of D26 (Figure 7). It should be noted that the pKa of benzylamine is 9.3, rendering the 3′-amine in N-debenzoyl-2′-deoxy-PTX positively charged in aqueous solutions at neutral pH. It is therefore somewhat surprising that the positively charged amine is repulsed from the carboxylate-containing binding site rather than attracted to it. It may be that the overall hydrophobicity of the binding overwhelms any advantage that would be attained from a salt bridge between the ammonium ion and the anionic side chain. To test this hypothesis, simulations were also

performed with a neutral 3′-amine on the ligand. In this case no flipping of the amino group was observed.

## DISCUSSION

Multiple structure-activity studies have demonstrated the importance of the 2′-OH group of PTX for its microtubule assembly and anticancer activity. It was recognized more than 25 years ago that acylation of the 2′-OH group results in loss of PTX's tubulin activity.(36) Replacement of the 2′-OH group with other functional groups yields inactive molecules, even if the proper stereochemistry is retained. All of the prior investigations into the role of this substitutent in the PTX-tubulin interaction relied on tubulin polymerization or cytotoxicity assays for activity data, which are valuable but do not specifically assess binding site interactions. In this work the role of the 2′-OH in the energetics of the PTX-tubulin complex has been directly examined through quantitative analysis of truncated derivatives of PTX.

The affinity of 2′-deoxy-PTX for GMPcPP-microtubules is two orders of magnitude lower than the affinity of PTX for microtubules. This corresponds to a difference in standard free energy of binding between the two ligands of about 3 kcal/mol, which is reasonable for removal of a hydrogen bonding interaction between the ligand and the receptor. Removal of the rest of the side chain has a relatively minor effect on complex formation: the affinity of 2′-deoxy-PTX for GMPcPP-microtubules is only about 3-fold higher than the affinity of baccatin III for microtubules and the standard free energies of binding for the two ligands differ by about 0.7 kcal/mol. Thus, 80% of the contribution of the entire C-13 side chain to the stability of the PTX-tubulin complex can be attributed to the 2′-OH group.

This analysis does not consider the change in ligand conformational entropy that should occur when the PTX side chain is immobilized in the binding site, which will affect PTX and 2′-deoxy-PTX but not baccatin III binding to microtubules. We believe that the conformational entropy differences between the molecules are not large enough to alter our conclusions. Buey *et al.* determined thermodynamic parameters for PTX binding to crosslinked microtubules by measuring the apparent equilibrium constant as a function of temperature (37). At 37 °C the association is entropically unfavored by about −2 ± 1 kcal/mol ($\Delta S^{\circ}_{app} = -29.3 \pm 13.1$ J/mol·K). Since there are a number of species that can undergo entropic changes upon ligand binding to microtubules, including protein moieties and water molecules, the contribution of the side chain cannot be extracted from the overall value. But in view of the fact that the unfavorable entropy change is a relatively small contribution to the overall free energy of binding for the entire PTX molecule ($\Delta H^{\circ}_{app} = -12.3 \pm 1.0$ kcal/mol and $\Delta G^{\circ}_{app} = -10.0 \pm 0.05$ kcal/mol at 37 °C), the differences in ligand conformational entropies should also be minor contributors to the overall binding energetics of the ligands.

The relative differences in binding free energies for the ligands are also reflected in their efficacies. The effect of taxane binding on tubulin assembly is assessed by the ligand's effect on tubulin critical concentration, which can be converted into an apparent standard free energy of elongation. Of the 1 kcal/mol difference between the elongation free energies PTX and baccatin III induced tubulin assembly, 0.7 kcal/mol can be attributed to the 2′-OH. These numbers must be interpreted cautiously, however, since the PTX binding site is only partially occupied under the experimental conditions. Nevertheless, these data show the same trend as the binding site affinities: removal of just the 2′-OH produces a molecule with efficacy that is more similar to that of baccatin III than to that of PTX as a promoter of tubulin assembly. Cellular effects of the three ligands parallel the in vitro tubulin results. Baccatin III is about 3.3 log units less active than PTX, and 2′-deoxy-PTX is 2.6 log units

less active than PTX. Again, about 80% of the difference in the activities of baccatin III and PTX can be attributed to the 2′-OH.

Coupling these results with fact that changing the substituents on the 3′-amide and 3′-carbon produces only minor alterations in the affinity and activity of taxanes (38, 39), we hypothesize that the primary role of the rest of the side chain is to properly position the 2′-OH group to donate a hydrogen bond to the receptor site.

Energy minimization revealed three candidates for the hydrogen bond acceptor in the PTX binding site: the amide nitrogens of R369 and G370, and the carboxylate of D26. Interestingly, molecular dynamics simulations identified different hydrogen bond acceptors with the two initial structures. One interpretation of these results is that the hydrogen bonds can fluctuate between the various acceptors, which seem to be the backbone amide nitrogens in the 1JFF structure and the carboxylate oxygens in the T-Taxol structure. If these results are considered in light of biochemical data, a different picture emerges. Himes and coworkers have performed a number of elegant experiments using site directed mutagenesis on yeast tubulin. Tubulin from *Saccharomyces cerevisiae* is insensitive to PTX, and no binding to microtubules formed from the wild type protein has been observed (40). Five residues in the PTX binding site are different in mammalian and yeast tubulin: K19, V23, D26, H227 and F270 in mammalian beta tubulin are replaced with A19, T23, G26, N227 and Y270 in yeast. When these five residues in yeast are mutated to the mammalian amino acids, the modified protein binds PTX. (41) Subsequent study of mutants with four of the five yeast amino acids changed to their mammalian counterparts indicate that K19 or H227 can be substituted with A or N, respectively, without loss of PTX binding. Mutants that possess the yeast amino acid at V23, D26 or F270, however, are unable to bind PTX. Entwistle *et al.* propose that the F207Y mutation places a hydrophilic group in a hydrophobic pocket, close to the *p*-carbon on the C-3′-phenyl ring, such that both steric and electronic factors of the substitution are responsible for the lack of observed PTX binding to this mutant (42). The V23T mutation replaces a methyl group with a hydroxyl, which would provide a less favorable environment for the other aromatic ring on the side chain (3′-N-benzoyl). We propose that the deleterious effect of the D26G mutation is due to the loss of the important hydrogen bonding interaction with the 2′-OH rather than to loss of van der Waals interaction between the side chain methylene and the aromatic ring of the 3′-N-benzoyl substituent.

Other biological data support the importance of D26 in the PTX binding site on tubulin. A PTX-resistant KB-3-1 line that had an D26E mutation in β-tubulin also had microtubules that are less stable than those of the unexposed cells (43). It is not known, however, if the mutated tubulin had an altered affinity for PTX.

Gueritte-Voegelein *et al.* (44) found that that the removal of the N-benzoyl group causes 94% loss in tubulin assembly activity of PTX. We find here that the removal of the N-benzoyl group causes complete loss in tubulin-assembly activity as well as the cytotoxicity and the microtubule-affinity of 2′-deoxy-PTX. This could be attributed to the loss of hydrophobic interactions as suggested by Bode et al. (40) between the N-benzoyl group and methylene groups of V23, K19 and D26 (5). However, computational simulations with PTX in 1JFF and N-debenzoyl-2′-deoxy-PTX created from PTX in 1JFF reveal that the removal of N-benzoyl group causes the flipping of the unsubstituted 3′-amino group to the exterior of the receptor site. Flipping was also observed upon simulations of PTX in T-Taxol-tubulin structure and N-debenzoyl-2′-deoxy-PTX created from PTX in T-Taxol-tubulin structure (data not shown). We therefore propose that the removal of N-benzoyl group not only removes the anchoring interactions between this group and the protein but it essentially

renders the conformation of the C-13 side chain destructive to the overall activity of the PTX derivative.

## SUMMARY AND CONCLUSIONS

The quantitative contribution of 2′-OH group as well as the function of N-benzoyl group in the association of PTX with microtubules has been studied. Removal of this group decreases the affinity, efficacy and cytotoxicity of the taxane almost as much as deleting the entire C-13 side chain of PTX. The importance of 2′-OH group in the C-13 side chain is attributed to its ability to form hydrogen bond with the residue D26 on β-tubulin. It can therefore be said that this hydrogen bonding interaction is the most important interaction that PTX forms with protein in the region of C-13 side chain. We propose that the hydrophobic substituents on the C-3′ carbon and amide nitrogen function primarily to hold the side chain in a conformation conducive to the formation of a productive hydrogen bonding interaction between the 2′-OH group and the protein.

## Acknowledgments

We gratefully acknowledge the computational resources provided by the University at Buffalo's Center for Computational Research (www.ccr.buffalo.edu) and the NYS Grid (www.nysgrid.org) as well as the assistance of Jon Bednasz (Center for Computational Research at SUNY Buffalo), Michael Lewis (Binghamton University), and Kenneth Chiu (Binghamton University). We are thankful to Dr. Dennis McGee (Binghamton University) for use of his cell culture facility and Mr. Colby Chiauzzi for participating in the modeling. The work was supported by NIH Grant CA-69571.

## Abbreviations

| | |
|---|---|
| **DMSO** | dimethyl sulfoxide |
| **EGTA** | ethylene glycol-bis(2-aminoethylether)-*N,N,N′,N′*-tetraacetic acid |
| **G-50** | Sephadex G-50 |
| **GDP** | guanosine 5′-diphosphate |
| **GMPcPP** | guanylyl-(α, β,)-methylene-diphosphonate |
| **GTP** | guanosine 5′-triphosphate |
| **$MgSO_4$** | magnesium sulfate |
| **N-AB-PT** | 3′-*N*-*m*-aminobenzamido-3′-*N*-debenzamidopaclitaxel |
| **PTX** | paclitaxel, Taxol® |
| **PIPES** | piperazine-N,N′-bis(2- ethanesulfonic acid) |
| **PME** | 100 mM PIPES, 1 mM $MgSO_4$, and 2 mM EGTA, pH 6.90 at 25 °C |

## References

1. Jordan MA, Wilson L. Microtubules as a target for anticancer drugs. Nature Rev Cancer. 2004; 4:253–265. [PubMed: 15057285]
2. Manfredi JJ, Horwitz SB. Taxol - an Antimitotic Agent with a New Mechanism of Action. Pharmacol Ther. 1984; 25:83–125. [PubMed: 6149569]
3. Dumontet C, Jordan MA. Microtubule-binding agents: a dynamic field of cancer therapeutics. Nature Rev Drug Disc. 2010; 9:790–803.
4. Nogales E, Wolf SG, Downing KH. Structure of the alpha beta tubulin dimer by electron crystallography. Nature. 1998; 391:199–203. [PubMed: 9428769]

5. Snyder JP, Nettles JH, Cornett B, Downing KH, Nogales E. The binding conformation of Taxol in beta-tubulin: A model based on electron crystallographic density. Proc Natl Acad Sci U S A. 2001; 98:5312–5316. [PubMed: 11309480]
6. Ganesh T, Guza RC, Bane S, Ravindra R, Shanker N, Lakdawala AS, Snyder JP, Kingston DGI. The bioactive Taxol conformation on beta-tubulin: Experimental evidence from highly active constrained analogs. Proc Natl Acad Sci USA. 2004; 101:10006–10011. [PubMed: 15226503]
7. Shanker N, Kingston DGI, Ganesh T, Yang C, Alcaraz AA, Geballe MT, Banerjee A, McGee D, Snyder JP, Bane S. Enhanced microtubule binding and tubulin assembly properties of conformationally constrained paclitaxel derivatives. Biochemistry. 2007; 46:11514–11527. [PubMed: 17892304]
8. Canales A, Rodriguez-Salarichs J, Trigili C, Nieto L, Coderch C, Andreu JM, Paterson I, Jimenez-Barbero J, Diaz JF. Insights into the interaction of Discodermolide and Docetaxel with Tubulin. Mapping the Binding Sites of Microtubule-Stabilizing Agents by Using an Integrated NMR and Computational Approach. ACS Chem Biol. 2011; 6:789–799. [PubMed: 21539341]
9. Yang Y, Alcaraz AA, Snyder JP. The Tubulin-Bound Conformation of Paclitaxel: T-Taxol vs "PTX-NY". J Nat Prod. 2009; 72:422–429. [PubMed: 19267457]
10. Sun L, Simmerling C, Ojima I. Recent Advances in the Study of the Bioactive Conformation of Taxol. ChemMedChem. 2009; 4:719–731. [PubMed: 19360801]
11. Ojima I, Chen J, Sun L, Borella CP, Wang T, Miller ML, Lin SN, Geng XD, Kuznetsova LR, Qu CX, Gallager D, Zhao XR, Zanardi I, Xia SJ, Horwitz SB, Mallen-St Clair J, Guerriero JL, Bar-Sagi D, Veith JM, Pera P, Bernacki RJ. Design, synthesis, and biological evaluation of new-generation taxoids. J Med Chem. 2008; 51:3203–3221. [PubMed: 18465846]
12. Jimenez-Barbaro J, Souto AA, Abal M, Barasoain I, Evangelio JA, Acuna AU, Andreu JM, Amat-Guerri F. Effect of 2′-OH acetylation on the bioactivity and conformation of 7-O-N-(4′-fluoresceincarbonyl)-L-alanyl taxol. A NMR-fluorescence microscopy study. Bioorg Med Chem. 1998; 6:1857–1863. [PubMed: 9839015]
13. Kant J, Huang S, Wong H, Fairchild C, Vyas D, Farina V. Sutdies toward structure-activity-relationships of Taxol®-Synthesis and cutotoxicity of Taxol® analogs with C-2′ modified phenylisoserine side-chains. Bioorg Med Chem Lett. 1993; 3:2471–2474.
14. Qi X, Lee SH, Yoon J, Lee YS. Synthesis of novel taxoid analogue containing sulfur group on C-13 side-chain: 2′-deoxy-2′-epi-mercaptopaclitaxel. Tetrahedron. 2003; 59:7409–7412.
15. Lowe J, Li H, Downing KH, Nogales E. Refined structure of alpha beta-tubulin at 3.5 A resolution. J Mol Biol. 2001; 313:1045–1057. [PubMed: 11700061]
16. Walker K, Fujisaki S, Long R, Croteau R. Molecular cloning and heterologous expression of the C-13 phenylpropanoid side chain-CoA acyltransferase that functions in Taxol biosynthesis. Proc Natl Acad Sci USA. 2002; 99:12715–12720. [PubMed: 12232048]
17. Long RM, Lagisetti C, Coates RM, Croteau R. Specificity of the *N*-Benzoyl Transferase Responsible for the Last Step of Taxol Biosynthesis. Arch Biochem Biophys. 2008; 477:384–389. [PubMed: 18621016]
18. Li YK, Poliks B, Cegelski L, Poliks M, Gryczynski Z, Piszczek G, Jagtap PG, Studelska DR, Kingston DGI, Schaefer J, Bane S. Conformation of microtubule-bound paclitaxel determined by fluorescence spectroscopy and REDOR NMR. Biochemistry. 2000; 39:281–291. [PubMed: 10630987]
19. Diaz JF, Andreu JM. Assembly of purified GDP-tubulin into microtubules induced by taxol and taxotere - reversibility, ligand stoichiometry, and competition. Biochemistry. 1993; 32:2747–2755. [PubMed: 8096151]
20. Chatterjee SK, Barron DM, Vos S, Bane S. Baccatin III induces assembly of purified tubulin into long microtubules. Biochemistry. 2001; 40:6964–6970. [PubMed: 11389612]
21. Williams RC Jr, Lee JC. Preparation of tubulin from brain. Meth Enzymol. 1982; 85(Pt B):376–385. [PubMed: 7121276]
22. Penefsky HS. A centrifuged-column procedure for the measurement of ligand binding by beef heart F1. Meth Enzymol. 1979; 56:527–530. [PubMed: 156867]
23. Li YK, Edsall R, Jagtap PG, Kingston DGI, Bane S. Equilibrium studies of a fluorescent paclitaxel derivative binding to microtubules. Biochemistry. 2000; 39:616–623. [PubMed: 10642187]

24. Seckler R, Wu GM, Timasheff SN. Interactions of tubulin with guanylyl-(beta-gamma-methylene)diphosphate - Formation and assembly of a stoichiometric complex. J Biol Chem. 1990; 265:7655–7661. [PubMed: 2332445]
25. Sharma S, Ganesh T, Kingston D, Bane S. Promotion of tubulin assembly by poorly soluble taxol analogs. Anal Biochem. 2007; 360:56–62. [PubMed: 17097592]
26. Skehan P, Storeng R, Scudiero D, Monks A, McMahon J, Vistica D, Warren JT, Bokesch H, Kenney S, Boyd MR. New Colormetric Cytotoxicity Assay for Anticancer-Drug Screening. J Natl Cancer Inst. 1990; 82:1107–1112. [PubMed: 2359136]
27. Alcaraz AA, Mehta AK, Johnson SA, Snyder JP. T-taxol conformation. J Med Chem. 2006; 49:2478–2488. [PubMed: 16610791]
28. Singh UC, Kollman PA. An Approach to Computing Electrostatic Charges for Molecules. J Comp Chem. 1984; 5:129–145.
29. Jorgensen WL, Chandrasekhar J, Madura JD, Impey RW, Klein ML. Comparison of simple potential functions for simulating liquid water. J Chem Phys. 1983; 79:926–935.
30. Diaz JF, Menendez M, Andreu JM. Thermodynamics of ligand-induced assembly of tubulin. Biochemistry. 1993; 32:10067–10077. [PubMed: 8104479]
31. Diaz JF, Strobe R, Engelborghs Y, Souto AA, Andreu JM. Molecular recognition of Taxol by microtubules - Kinetics and thermodynamics of binding of fluorescent Taxol derivatives to an exposed site. J Biol Chem. 2000; 275:26265–26276. [PubMed: 10818101]
32. Han Y, Chaudhary AG, Chordia MD, Sackett DL, PerezRamirez B, Kingston DGI, Bane S. Interaction of a fluorescent derivative of paclitaxel (Taxol) with microtubules and tubulin-colchicine. Biochemistry. 1996; 35:14173–14183. [PubMed: 8916903]
33. Diaz JF, Buey RM. Characterizing ligand-microtubule binding by competition methods. Meth Mol Med. 2007; 137:245–260.
34. Andreu JM, Barasoain I. The interaction of baccatin III with the taxol binding site of microtubules determined by a homogeneous assay with fluorescent taxoid. Biochemistry. 2001; 40:11975–11984. [PubMed: 11580273]
35. Timasheff SN, Grisham LM. In vitro assembly of cytoplasmic microtubules. Annual Review of Biochemistry. 1980; 49:565–591.
36. Mellado W, Magri NF, Kingston DGI, Garcia-Arenas R, Orr GA, Horwitz SB. Preparation and Biological Activity of Taxol Acetates. Biochem Biophys Res Comm. 1984; 124:329–336. [PubMed: 6548627]
37. Buey RM, Barasoain I, Jackson E, Meyer A, Giannakakou P, Paterson I, Mooberry S, Andreu JM, Diaz JF. Microtubule interactions with chemically diverse stabilizing agents: Thermodynamics of binding to the paclitaxel site predicts cytotoxicity. Chem Biol. 2005; 12:1269–1279. [PubMed: 16356844]
38. Matesanz R, Barasoain I, Yang CG, Wang L, Li X, De Ines C, Coderch C, Gago F, Barbero JJ, Andreu JM, Fang WS, Diaz JF. Optimization of taxane binding to microtubules: Binding affinity dissection and incremental construction of a high-affinity analog of paclitaxel. Chem Biol. 2008; 15:573–585. [PubMed: 18559268]
39. Fu Y, Li S, Zu Y, Yang G, Yang Z, Luo M, Jiang S, Wink M, Efferth T. Medicinal Chemistry of Paclitaxel and its Analogues. Curr Med Chem. 2009; 16:3966–3985. [PubMed: 19747129]
40. Bode CJ, Gupta ML, Reiff EA, Suprenant KA, Georg GI, Himes RH. Epothilone and paclitaxel: Unexpected differences in promoting the assembly and stabilization of yeast microtubules. Biochemistry. 2002; 41:3870–3874. [PubMed: 11900528]
41. Gupta ML, Bode CJ, Georg GI, Himes RH. Understanding tubulin-Taxol interactions: Mutations that impart Taxol binding to yeast tubulin. Proc Natl Acad Sci USA. 2003; 100:6394–6397. [PubMed: 12740436]
42. Entwistle RA, Winefield RD, Foland TB, Lushington GH, Himes RH. The paclitaxel site in tubulin probed by site-directed mutagenesis of Saccharomyces cerevisiae beta-tubulin. FEBS Letters. 2008; 582:2467–2470. [PubMed: 18570892]
43. Hari M, Loganzo F, Annable T, Tan XZ, Musto S, Morilla DB, Nettles JH, Snyder JP, Greenberger LM. Paclitaxel-resistant cells have a mutation in the paclitaxel-binding region of beta-tubulin

(Asp(26)Glu) and less stable microtubules. Mol Cancer Ther. 2006; 5:270–278. [PubMed: 16505100]

44. Gueritte-Voegelein F, Guenard D, Lavelle F, Legoff MT, Mangatal L, Potier P. Relatioships between the structure of taxol analogs and their antimitotic activity. J Med Chem. 1991; 34:992–998. [PubMed: 1672159]

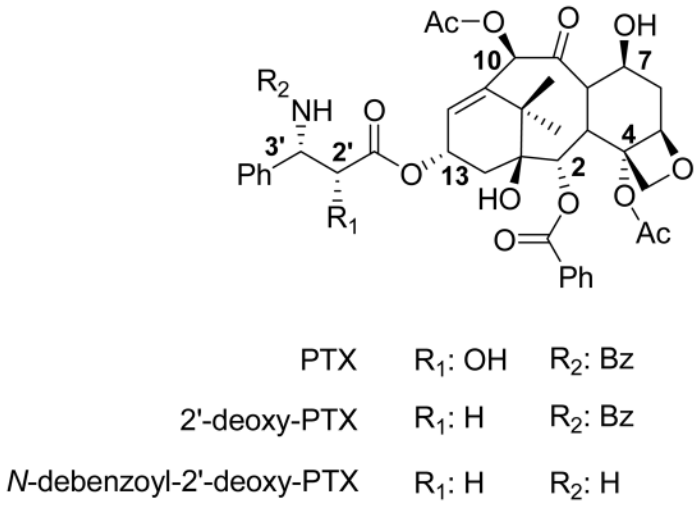


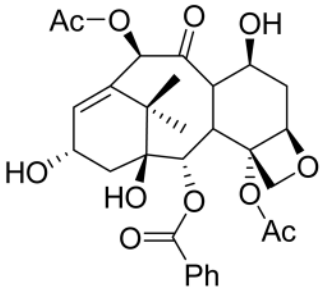


Baccatin III

| | | |
|---|---|---|
| PTX | $R_1$: OH | $R_2$: Bz |
| 2'-deoxy-PTX | $R_1$: H | $R_2$: Bz |
| *N*-debenzoyl-2'-deoxy-PTX | $R_1$: H | $R_2$: H |

**Figure 1.**
Structure of PTX and deletion analogs.

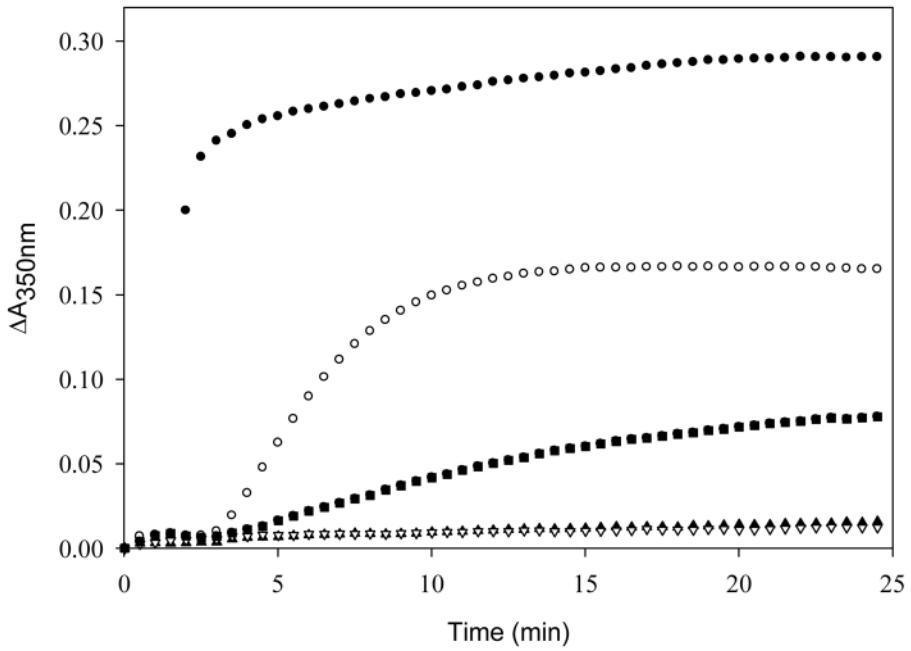


**Figure 2.**

Effect of taxanes on tubulin assembly. Tubulin (5 μM) was treated with 15 μM of PTX (○), 2′-deoxy-PTX (●), *N*-debenzoyl-2′-deoxy-PTX (▲), baccatin III (■) or no drug (▽). Experiments were performed in PME buffer containing 0.1 mM GTP and 4% DMSO at 37 °C as described under *Materials and Methods*. Assembly was monitored by increase in apparent absorption at 350 nm.

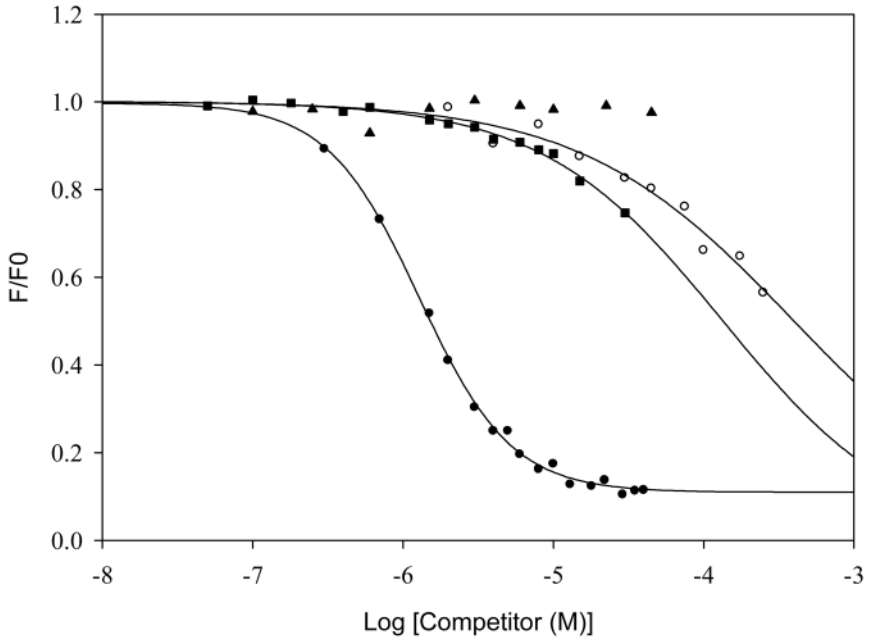


**Figure 3.**

Competition binding curves for taxanes binding to GMPcPP microtubules. PTX (●), 2′-deoxy-PTX (■), N-debenzoyl-2′-deoxy-PTX (▲) or baccatin III (○) in DMSO were added to solutions of GMPcPP microtubules (1 μM) containing N-AB-PT (1 μM). The samples were incubated at 37 °C for 30 min and the emission intensity of N-AB-PT was recorded for each sample as described under *Materials and Methods*. The concentration of DMSO was maintained at 15%.

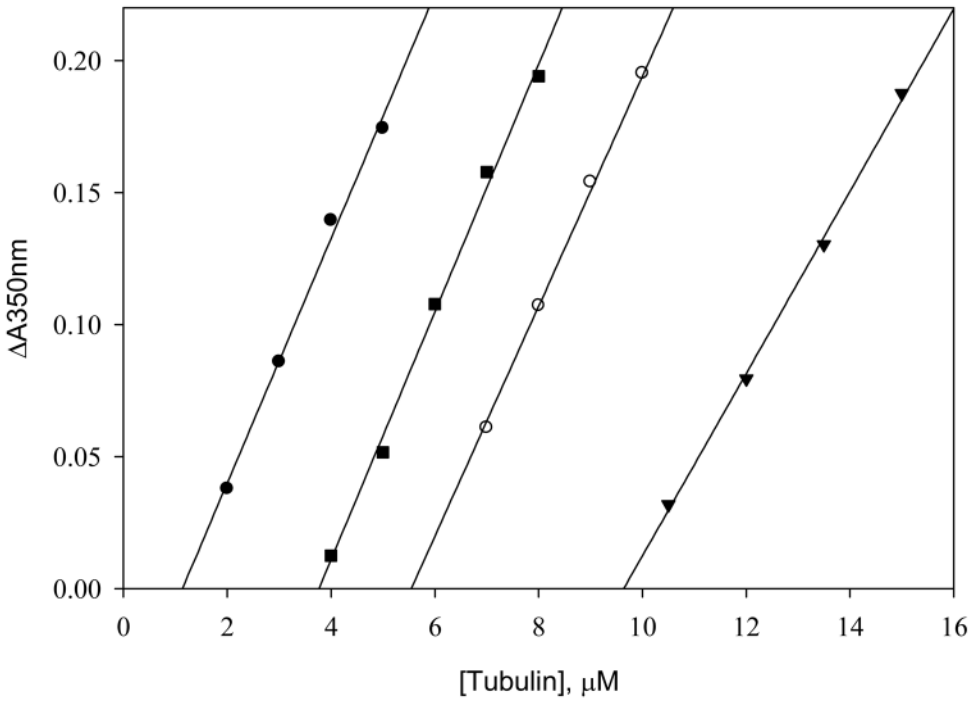


**Figure 4.**

Critical concentration of tubulin assembly in the presence of taxanes. PTX (●), 2′-deoxy-PTX (■), baccatin III (○) and 4 % DMSO (▼) were used to assemble varying concentrations of tubulin at 37 °C as described under *Materials and Methods*. Taxane:tubulin ratios were maintained at 1:0.5, 1:1 and 1:1.3 for PTX, 2′-deoxy-PTX and baccatin III, respectively. The extent of assembly was measured by increase in apparent absorption at 350 nm ($\Delta A_{350nm}$). The critical concentration was obtained from the x-intercept of each plot.

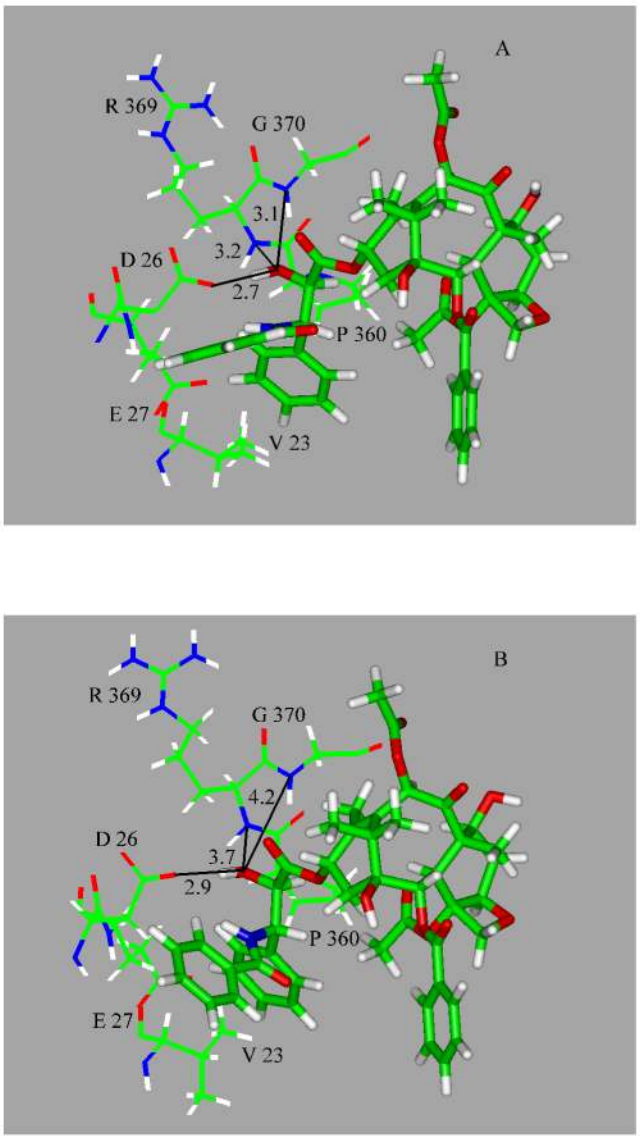


**Figure 5.**

Illustration of PTX bound to tubulin in minimized structures from initial coordinates of 1JFF (A) or T-Taxol (B). Residues within 6Å of the 2′-OH group are labeled. Distances between the oxygen of the 2′-OH and potential hydrogen bond acceptors (carboxylic acid of D26, backbone amides of G370 and R369) are shown by solid lines.

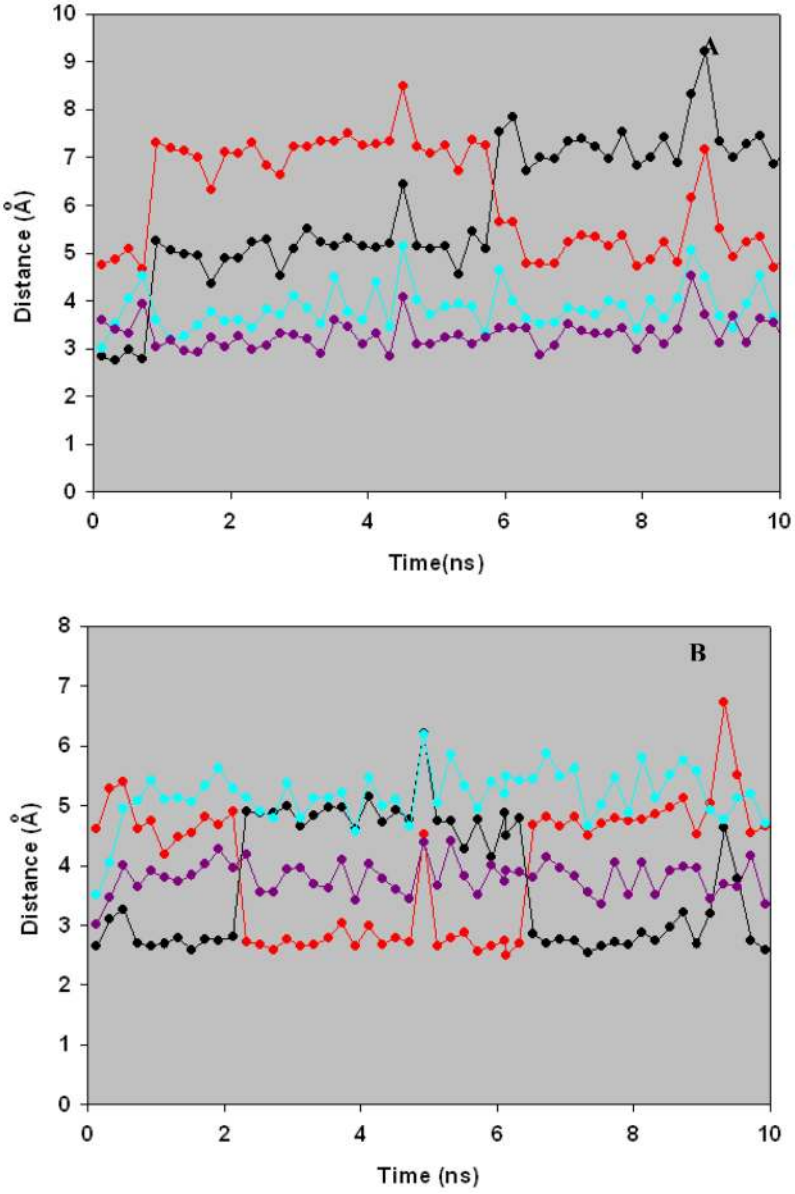


**Figure 6.**

Time evolution of the distances between the 2′-OH group of PTX and selected atoms in the protein during dynamics. The structures from Figure 5 were subjected to 10 ns dynamic run using AMBER 9 at 300K as described under *Materials and Methods*. Distances between the oxygen of the 2′-OH and the carboxylate oxygens of D26 ( —●— —●—), the nitrogen atoms of the backbone amides of G370 ( —●—) and R369 ( —●—) are shown. (A) Long term dynamics of 1JFF. (B) Long term dynamics of T-Taxol-tubulin structure.

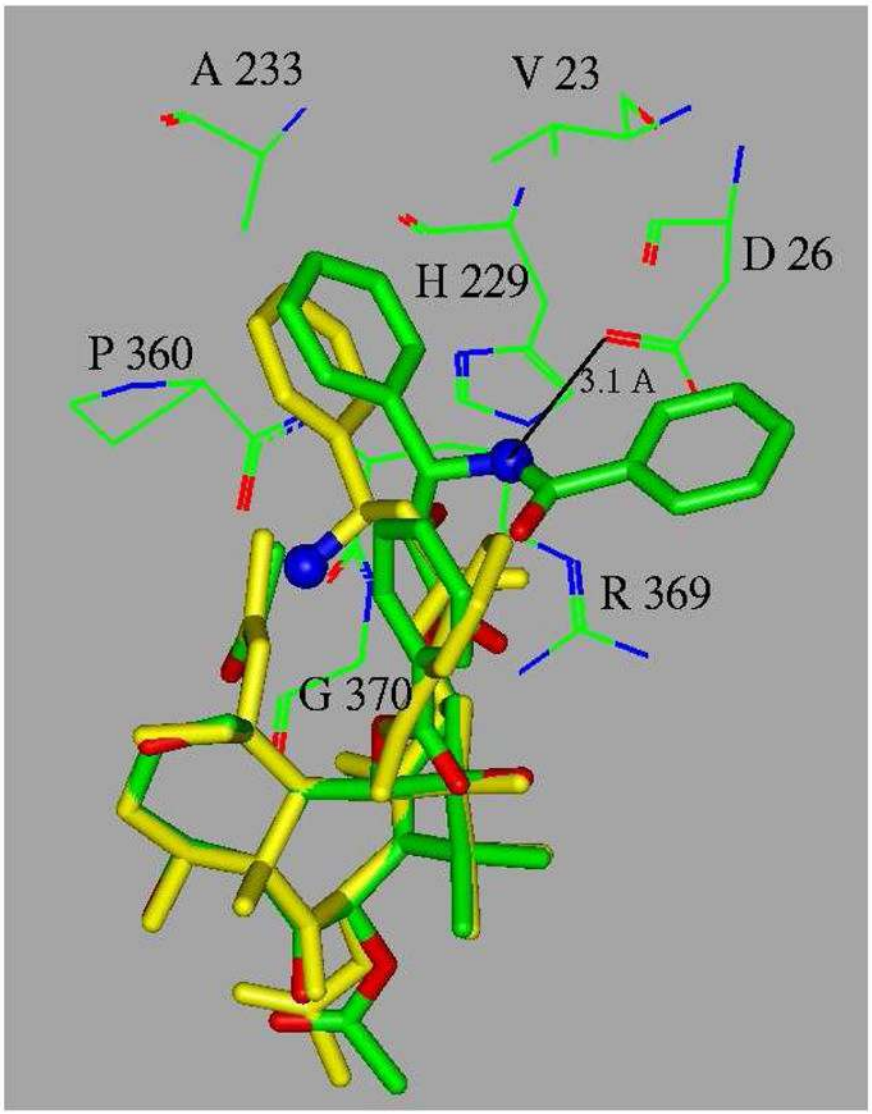


**Figure 7.**

Schematic diagram of β-subunit showing microtubule binding site within 6Å of the 3′-nitrogen of PTX in 1JFF. The 3′-nitrogen of PTX (green) and that of *N*-debenzoyl-2′-deoxy-PTX (yellow) are shown as blue balls. *N*-debenzoyl-2′-deoxy-PTX was created from PTX in 1JFF by removing the 2′-OH group and the N-benzoyl group. The resulting structure was equilibrated and minimized and superimposed with respect to the baccatin core on PTX in equilibrated and minimized 1JFF structure. The side chain of D26 was found at 3.1Å (shown by the black line) from the 3′-nitrogen of PTX.

## Table 1

Equilibrium Binding Parameters for Taxanes Binding to GMPcPP-Microtubules[a]

| Taxane | $Ka_{app}$ ($\times 10^6$ $M^{-1}$)[b] | $\Delta G^\circ$ (kcal/mol)[c] |
|---|---|---|
| PTX | 53 ± 2 | −11 ± 0.02 |
| 2′-deoxy-PTX | 0.50 ± 0.01 | −8.1 ± 0.01 |
| Baccatin III | 0.17 ± 0.03 | −7.4 ± 0.09 |
| *N*-debenzoyl-2′-deoxy-PTX | - | - |

[a] All measurements were performed at 37 °C as described under *Materials and Methods*.

[b] Apparent equilibrium constant for taxane binding to GMPcPP microtubules.

[c] Apparent standard free energy change associated with binding of ligands to GMPcPP-microtubules.

## Table 2

Effect of Taxanes on the Critical Concentration of Tubulin Assembly

| Agent | $C_{crit}$ (μM)[a] | Kp (× $10^5$ $M^{-1}$)[b] | $\Delta G^\circ_{app}$ (kcal/mol)[c] |
|---|---|---|---|
| PTX | 1.1 ± 0.1 | 9.1 ± 0.1 | −8.4 ± 0.06 |
| 2′-deoxy-PTX | 3.7 ± 0.2 | 2.7 ± 0.1 | −7.7 ± 0.03 |
| Baccatin III | 5.6 ± 0.2 | 1.8 ± 0.05 | −7.4 ± 0.02 |
| 2 % DMSO | 9.6 ± 0.5 | 1.0 ± 0.05 | −7.1 ± 0.03 |

[a] Critical concentration of tubulin assembly at 37 °C.

[b] Apparent equilibrium constant for microtubule growth at 37 °C, $K_p = 1/C_{crit}$.

[c] Apparent standard free energy change at steady state.

## Table 3

Cytotoxicity of Taxanes for PC3 Cells

| Taxane | $IC_{50}$ (nM) | log($IC_{50}$) |
|---|---|---|
| PTX | 1.41 ± 0.32 | −8.8 |
| 2′-deoxy-PTX | 526 ± 82 | −6.3 |
| Baccatin III | ~ 3000 | ~ −5.5 |
| *N*-debenzoyl-2′-deoxy-PTX | >10,000[a] | |

Cytotoxicities of ligands were measured as described under *Materials and Methods*.

[a]No cytotoxicity observed at 10 μM, the highest concentration tested.